

## An anomalous X-ray scattering study of an aqueous solution of $\text{ZnCl}_2$

This article has been downloaded from IOPscience. Please scroll down to see the full text article.

1989 J. Phys.: Condens. Matter 1 8575

(<http://iopscience.iop.org/0953-8984/1/44/028>)

View [the table of contents for this issue](#), or go to the [journal homepage](#) for more

Download details:

IP Address: 171.66.16.96

The article was downloaded on 10/05/2010 at 20:50

Please note that [terms and conditions apply](#).

## An anomalous x-ray scattering study of an aqueous solution of $\text{ZnCl}_2$

E Matsubara and Y Waseda

Research Institute of Mineral Dressing and Metallurgy (SENKEN), Tohoku University, Sendai 980, Japan

Received 12 April 1989, in final form 13 June 1989

**Abstract.** Concentrated aqueous solutions of  $\text{ZnCl}_2$  have been studied by the anomalous x-ray scattering (AXS) technique at Zn K-absorption edge. The hydration number around  $\text{Zn}^{2+}$  was found to be 5.7 at a distance of 0.210 nm in the  $0.98 \text{ kmol m}^{-3}$   $\text{ZnCl}_2$  aqueous solution. On the other hand, in the  $2.85 \text{ kmol m}^{-3}$   $\text{ZnCl}_2$  aqueous solution the hydration number becomes 6.2 with a distance of 0.215 nm. The present study has demonstrated the capability of the AXS technique for structural study of aqueous solutions containing heavy metallic ions.

### 1. Introduction

The structure of concentrated aqueous solutions of various salts of divalent transition metals has been studied with some diffraction techniques, such as, x-ray scattering [1–4], neutron scattering [5, 6], Raman scattering [7], extended x-ray absorption fine structure (EXAFS) [8–11], and anomalous x-ray scattering (AXS) [10]. Howe and co-workers [5] determined a partial structure factor for nickel ion pairs, using a neutron scattering technique with isotope substitution and proposed the existence of strong correlations between nickel ions. However, this isotope substitution technique in neutron diffraction is limited to some particular systems, such as  $\text{NiCl}_2$  in aqueous solution. From Raman spectroscopy, it has been pointed out [7] that there is a tendency to complexes formation around divalent cations Zn, Cd and Ni in concentrated aqueous solutions.

The advantage of the EXAFS and AXS techniques is that chemical environment around a specific element in materials can be probed. In the conventional x-ray and neutron diffraction techniques, because of the lack of chemical selectivity, the details of a structure in aqueous solution are often difficult to obtain. For example, in a metal-halide aqueous solution, its total structure factor is described as a sum of ten partial structure factors. Thus, to determine the individual contributions is an extremely difficult and sometimes questionable procedure. Both the EXAFS and AXS techniques solve these problems. Although the EXAFS measurement is much easier than AXS, its analysis contains more theoretical ambiguity, such as the determination of back amplitudes and phase shifts (see for example [12]). It has been shown [9] by EXAFS that some local order, resembling that of the corresponding crystal, exists in highly concentrated solution of  $\text{ZnBr}_2$ ,  $\text{CuBr}_2$  and  $\text{CuCl}_2$  and this order decreases with decrease in concentration while the hydration number increases. EXAFS has also been applied [11] to several zinc halide

**Table 1.** Compositions and densities of the aqueous solutions used in the present measurements.

ZnCl <sub>2</sub> (kmol m <sup>-3</sup> )	Zn	Cl (at.%)	H	O	Added HClO <sub>4</sub> (kmol m <sup>-3</sup> )	Density (10 <sup>3</sup> kg m <sup>-3</sup> )
0.98	0.6	1.2	65.5	32.7	0.04	1.107
2.85	1.8	3.6	63.1	31.5	0.12	1.291

aqueous solutions and reported that the hydration number of Zn<sup>2+</sup> is about 6 to 7 at low concentrations of zinc halide up to 0.5 kmol m<sup>-3</sup> and decreases with concentration by replacing water molecules by halide ions. By the use of AXS as well as EXAFS, it has been concluded [10] that tetrahedral complexes about the Zn<sup>2+</sup> exist in ZnBr<sub>2</sub> aqueous solutions.

As synchrotron radiation sources of x-rays became more accessible, the AXS technique has become increasingly popular, although its application to aqueous solutions is still very limited. In this paper, we will explain the experimental procedure and data analysis for AXS, followed by the results of the AXS measurements in concentrated aqueous solutions of ZnCl<sub>2</sub>.

## 2. Experimental procedure

Two kinds of aqueous solutions of ZnCl<sub>2</sub> were prepared by dissolving the crystal in deionised water. Zn<sup>2+</sup> contents in the solutions were determined by titration with EDTA (ethylenediaminetetraacetic acid). A small amount of perchloric acid was added to all the solutions and made their pH kept at 3.0 in order to prevent hydrolysis of the metal ions. The reason why the perchloric acid was used is to avoid any increase in the amount of free chloride ions. The compositions of the solutions are summarised in table 1 with their densities determined with a pycnometer and the concentrations of the added perchloric acid.

Scattering data were collected at the Photon Factory (PF) of the National Laboratory for High-Energy Physics, Tsukuba, Japan, using the beam line 7C where a double Si(111) crystal monochromator is installed. The details of the experimental apparatus are described in [13]. Some additional details necessary for the present study are given below. Because of particular near-edge phenomena, such as x-ray absorption near-edge structure (XANES), EXAFS and extremely intense fluorescent radiation above the absorption edge, anomalous x-ray scattering data were measured at the energies below the Zn K-absorption edge. Intensity of the incident beam was monitored by a nitrogen-gas-flow type ion chamber placed in front of the sample. Measured intensity was converted to intensity in counts per photon by dividing the total number of photons estimated from the total monitor counts [14]. A portable pure germanium solid-state detector was used to ensure that the coherent intensity and Zn K $\alpha$  fluorescence from the solution were separately collected. The K $\beta$  fluorescence overlapping with the coherent intensity near the absorption edge was corrected [15] by subtracting the intensity of the K $\beta$  fluorescence estimated from the measured intensity of the K $\alpha$  fluorescence and the intensity ratio of K $\beta$  to K $\alpha$  [16]. The effect of higher harmonics diffracted by a Si(333) plane was reduced to an insignificant level by intentionally detuning the second crystal of the monochromator with a piezo-electric device attached to it.

Scattering intensity from the sample was collected using two different geometries, namely symmetrical reflection and transmission geometries. A deep cell with a window of a thin 'kapton' film over the solution was used for the measurements in the reflection geometry. In the reflection geometry, the contribution of scattering intensity from the window becomes very large at low scattering angles, which sometimes disturbs the accurate measurement of scattering intensity from the solution itself. Thus, in order to reduce the contribution from the window, intensity at the low angular region was measured in the transmission geometry, using a cell confined between thin kapton films. Thicknesses of the cells for the 0.98 and 2.85  $\text{kmol m}^{-3}$   $ZnCl_2$  solutions were 0.92 and 1.3 mm, respectively. Correction for the scattering by the window of the cell was made by measuring the intensities from the empty cell ( $I_c$ ) and the filled cell ( $I_s$ ), and using the following equations in each geometry. In transmission geometry

$$1/A_T [I_s - \exp(-\mu_s t_s I_c / \cos \theta)] \quad (1)$$

where

$$A_T = (t_s / \cos \theta) \exp[-(\mu_s t_s + 2\mu_c t_c) / \cos \theta]. \quad (2)$$

In the reflection geometry

$$(1/A_R)(I_s - I_c) \quad (3)$$

where

$$A_R = (1/2\mu_s) \exp[-(2\mu_c t_c / \sin \theta)] \quad (4)$$

Here,  $t_s$  and  $t_c$  are the thicknesses of the sample and kapton window,  $\mu_c$  and  $\mu_s$  are the linear absorption coefficients of the sample and the film, respectively, and  $\theta$  is the scattering angle. The products  $2\mu_c t_c$  and  $\mu_s t_s$  used in the analysis were determined experimentally by measuring the absorption of the empty and filled cells for the transmission geometry for each solution. The value of  $t_s$  was obtained by dividing the product by the value of the linear absorption coefficient of the solution  $\mu_s$  which was calculated from the concentration, density and tabulated mass-absorption coefficients [17]. Incidentally, the intensity contribution from the kapton window of 25  $\mu\text{m}$  thickness is about 5% or less in the transmission geometry and about 10 to 20% in the reflection geometry. Both the corrected intensities were combined for further analysis of the data.

The intensity of at least 40000 counts was collected at each scattering angle, the average being about 80000 counts. The corrected intensity was converted to electron units per atom by the generalised Krogh–Moe–Norman method [18], using the x-ray atomic scattering factors of  $Zn^{2+}$ ,  $Cl^-$ , H and O [19], including their anomalous dispersion terms [17] theoretically calculated by the method of Cromer and Liberman [20], and Compton scattering factors of  $Zn^{2+}$ ,  $Cl^-$  and O from [21] and H from [22] with so-called Breit–Dirac recoil factors. In the present work, the observed intensity data at  $Q$ -values  $< 2.5 \text{ nm}^{-1}$  have been smoothly extrapolated to  $Q = 0$ . The effect of the extrapolation and the truncation up to  $80 \text{ nm}^{-1}$  is known to give no critical contribution in the calculation of the RDF by Fourier transformation [23, 24].

The ordinary reduced RDF  $G(r)$  was evaluated in each solution, using the coherent intensity in electron units per atom,  $I_{cu}^{coh}(Q)$  determined at 9.361 keV.

**Table 2.** Sample parameters for the aqueous solutions of 0.98 and 2.85 kmol m<sup>-3</sup> ZnCl<sub>2</sub> (equation (14)).

ZnCl <sub>2</sub> (kmol m <sup>-3</sup> )	A	B	C	D
0.98	2.33	0.163	6.51	8.67
2.85	1.90	0.147	4.96	7.30

$$G(r) = \frac{2}{\pi} \int_0^{\infty} Qi(Q) \sin(Qr) dQ \quad (5)$$

in which

$$i(Q) = \left( I_{\text{eu}}^{\text{coh}}(Q) - \sum_{j=1}^n c_j f_j^2 \right) / \left( \sum_{j=1}^n c_j f_j \right). \quad (6)$$

where  $n$  is the number of the constituent elements, and  $f_j$  and  $c_j$  are the scattering factor and concentration of the  $j$ th element, respectively. Since the incident beam energy was selected at the lower energy side of the Zn K-absorption edge, the variation detected in intensity is attributed only to the change of the real part of the anomalous dispersion term  $f'$  of Zn. Thus, the difference between scattering intensities measured at two energies  $E_1$  and  $E_2$  ( $E_1 < E_2$ ) is given by

$$\Delta i(Q) = [I_{\text{eu}}^{\text{coh}}(Q, E_1) - \langle f^2(Q, E_1) \rangle] - [I_{\text{eu}}^{\text{coh}}(Q, E_2) - \langle f^2(Q, E_2) \rangle]. \quad (7)$$

The environmental reduced RDF around Zn,  $G_{\text{Zn}}(r)$ , is determined by the Fourier transform of the quantity  $Q\Delta i(Q)$

$$G_{\text{Zn}}(r) = \frac{2}{c_{\text{Zn}}(f'_{\text{Zn}}(E_1) - f'_{\text{Zn}}(E_2))} \int_0^{\infty} \frac{Q\Delta i(Q) \sin(Qr)}{W(Q)} dQ \quad (8)$$

and

$$W(Q) = \sum_{j=1}^n c_j \text{Re}[f_j(Q, E_1) + f_j(Q, E_2)]. \quad (9)$$

The function  $G_{\text{Zn}}(r)$  is also given by a sum of the reduced partial RDFs  $g_{\text{Zn}j}(r)$ .

$$G_{\text{Zn}}(r) + 4\pi r \rho_0 = g_{\text{ZnO}}(r) + g_{\text{ZnH}}(r) + g_{\text{ZnCl}}(r) + g_{\text{ZnZn}}(r) \quad (10)$$

where  $\rho_0$  is the average number density. These reduced partial RDFs are described with the number density of the constituent elements around Zn,  $\rho_{\text{Zn}j}(r)$ , namely

$$g_{\text{ZnO}}(r) = 4\pi r \sum_{j=1}^n \frac{\text{Re}[f_{\text{O}}(Q, E_1) + f_{\text{O}}(Q, E_2)]}{W(Q)} \rho_{\text{ZnO}}(r) \quad (11)$$

The functions  $g_{\text{ZnH}}(r)$ ,  $g_{\text{ZnCl}}(r)$  and  $g_{\text{ZnZn}}(r)$  are similarly defined. Consequently, the left-hand side of (10) is described, in the following, as a sum of the four partial number densities  $\rho_{ij}(r)$ ;

$$A\rho_{\text{ZnO}}(r) + B\rho_{\text{ZnH}}(r) + C\rho_{\text{ZnCl}}(r) + D\rho_{\text{ZnZn}}(r). \quad (12)$$

The values of these sample parameters,  $A$ ,  $B$ ,  $C$  and  $D$  are given in table 2, using

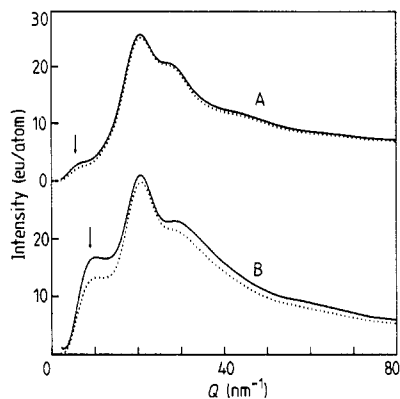


**Figure 1.** Intensity profiles ( $I_{\text{cu}}^{\text{coh}}$ ) measured at 9.361 (—) and 9.363 (⋯) keV for the aqueous solutions 0.98 (curves A) and 2.85  $\text{kmol m}^{-3}$  (curves B)  $\text{ZnCl}_2$ . Arrows indicate prepeaks.

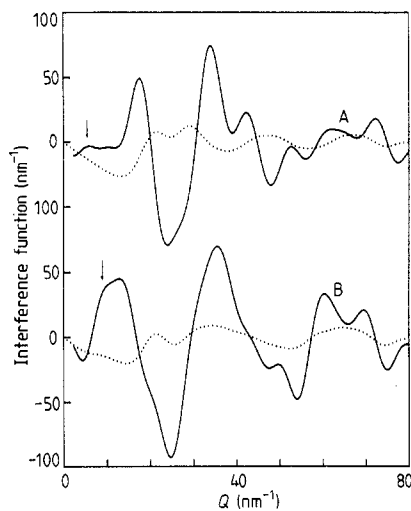


**Figure 2.** Intensity functions  $Q\Delta i(Q)$  (—) and  $Qi(Q)$  (⋯) for the aqueous solutions of 0.98 (curves A) and 2.85 (curves B)  $\text{kmol m}^{-3}$   $\text{ZnCl}_2$ . Arrows indicate the positions of the prepeaks in the observed intensities.

the average values of the scattering factors in the measured region ( $2.5 \text{ nm}^{-1} \leq Q \leq 80 \text{ nm}^{-1}$ ). The energy-derivative method with the AXS technique based upon the idea of Hosoya [25] and Shevchik [26] was first used by Fuoss and co-workers [27] with synchrotron radiation under the name of differential anomalous scattering (DAS), although the principle of the method itself is unchanged.

### 3. Results and discussion

Coherent intensity profiles ( $I_{\text{cu}}^{\text{coh}}$ ) of the 0.98 and 2.95  $\text{kmol m}^{-3}$   $\text{ZnCl}_2$  aqueous solutions are shown in figure 1. The full and dotted curves of each solution describe the scattering intensities at 9.361 and 9.636 keV, respectively, which correspond to energies of 299 and 24 keV below the Zn K-absorption edge (9.660 keV). These profiles essentially show typical profiles of aqueous solutions containing metallic ions, having a broad first peak at about  $20 \text{ nm}^{-1}$  with a shoulder at about  $30 \text{ nm}^{-1}$ . In addition to these ordinary features, there is a prepeak. A similar prepeak has been reported in some concentrated aqueous solutions such as  $\text{NiCl}_2$  [28]. The increase in the prepeak intensity and increase in its position with Zn concentrations in figure 1 are considered to be closely related to the ionic correlations in this solution. However, in order to understand the origin of this prepeak, a further structural analysis is essential, similar to that in [29] using the method of multipattern analysis based on neutron diffraction from isotopically enriched samples.

The differential intensity functions defined in (7) multiplied by  $Q$ ,  $Q\Delta i(Q)$  are shown in figure 2. For comparison, the ordinary intensity functions  $Qi(Q)$  obtained in the similar manner from the function  $i(Q)$  in (6) are also shown by dotted curves in the same figure. The profile of  $Q\Delta i(Q)$  also shows a broad peak at the prepeak position, which is indicated with an arrow. This is further convincing evidence to support the assumption

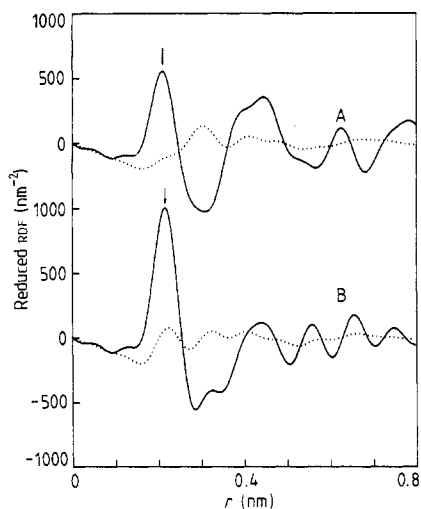


**Figure 3.** Environmental reduced radial distribution functions (RDFs) around the  $\text{Zn}^{2+}$ ,  $G_{\text{Zn}}(r)$  (—) for the aqueous solutions of 0.98 (curves A) and 2.85 (curves B)  $\text{kmol m}^{-3}$   $\text{ZnCl}_2$ . The ordinary reduced RDFs  $G(r)$ , are also shown ( $\cdots$ ). Arrows indicate the first peaks used for computation of the hydration numbers.

on the origin of the prepeak discussed above. Incidentally, it is interesting to notice that the differential intensity profile of the 2.85  $\text{kmol m}^{-3}$   $\text{ZnCl}_2$  aqueous solution in the bottom of this figure shows profile similar to the partial structure factor of Ni–Ni determined by Neilson and co-workers [28]. Fourier inversion of the differential intensity function  $Q\Delta i(Q)$  in (8) gives the environmental reduced RDF around Zn. The ordinary reduced RDF was similarly computed from the intensity function  $Qi(Q)$  and the results are shown in figure 3.

The peak is clearly detected in the ordinary reduced RDF of  $G(r)$  at about 0.3 nm. This peak is ascribed to the pairs of O–O and  $\text{Cl}^-$ –O because the distance between the oxygen atoms forming water molecules is 0.285 nm in liquid water [30] and the distance between O and  $\text{Cl}^-$  in the  $\text{Cl}^-$ – $\text{H}_2\text{O}$  conformation of the  $\text{NiCl}_2$  aqueous solution is 0.320 nm [31]. This peak completely disappears in the environmental RDF around Zn,  $G_{\text{Zn}}(r)$ . On the other hand, the first peak at about 0.2 nm in the  $G_{\text{Zn}}(r)$  is also visible in the  $G(r)$  as a shoulder or peak. The reported distances between  $\text{Zn}^{2+}$  and O in the  $\text{Zn}^{2+}$ – $\text{OH}_2$  conformation are about 0.2 nm. These are summarised in table 3. Furthermore, in the present AXS measurements, more than 90% of the total contribution is attributed to the pairs of  $\text{Zn}^{2+}$  and the O of the water molecule and the rest is attributed to the pairs of  $\text{Zn}^{2+}$  and H of the water molecule in a near-neighbour region around hydrogenated zinc ions. Thus, by assuming only the  $\text{Zn}^{2+}$  and O pairing, the hydration number of  $\text{Zn}^{2+}$  was calculated from the area under the first peak. It is known that no unique procedure is available, at the present time, for estimating the experimental uncertainty of the coordination number calculated from the RDF data. Thus, the error of this coordination number due to counting statistics in the intensity measurements was estimated using the method employed in the previous work of disordered system [32]. The resultant values in both solutions are also given in table 3. The following comments may also be suggested, regarding the error of the coordination number. A source of systematic errors for liquid structure by x-ray diffraction arises from the uncertainties of the atomic scattering factors and of the Compton scattering. According to the detailed discussion given in [33], the maximum error in these quantities is estimated less than 1% for the constituent elements presently investigated. Therefore, the total experimental uncertainty of the coordination number calculated in this work does not exceed the variation due to the counting statistics

**Table 3.** Summary of coordination numbers  $N$  and distances  $r$  in the concentrated aqueous solutions of various zinc salts.

Salts	Molarity ( $\text{kmol m}^{-3}$ )	$r$ (nm)	$N$	Method	Reference
$ZnCl_2$	0.98	0.210	$5.7 \pm 0.7$ O	AXS	Present work
	2.85	0.215	$6.2 \pm 0.2$ O	AXS	
$ZnCl_2$	0.5	0.205	5.7 O	EXAFS	[11]
		1	0.202		
	2	0.234	0.9 $Cl^-$		
		0.203	4.2 O		
$Zn(ClO_4)_2$	2.89	0.208	6 O	x-ray	[3]
	2.80	0.208	6 O	x-ray	[3]
$Zn(NO_3)_2$	1.0	0.209	6.2 O	x-ray	[34]
$ZnBr_2$	1.29	0.194	5–6 O	x-ray	[9]
		0.237	2 $Br^-$		
	3.23	0.194	4.5 O		
$ZnBr_2$	2.66	0.237	3 $Br^-$	EXAFS and AXS	[10]
		0.195	2.4 O		
		0.237	1.8 $Br^-$		

given in table 3. We could also suggest that the accuracy for the relative change in intensity arising from the energy dependence of the anomalous scattering terms is about an order of magnitude better than that of the usual intensity measurements, as already discussed [17, 26]. This includes the present case.

All of the recent EXAFS results indicate the existence of tetrahedral complexes about  $Zn^{2+}$  in concentrated aqueous solutions. Lagarde and co-workers [9] proposed a mixture of  $ZnBr_4$  tetrahedral complexes and hydrated free  $Zn^{2+}$  ions. The formation of tetrahedral complexes has also been suggested, consisting of 2.4  $Br^-$  and 1.2  $O^-$  atoms on average [10]. However, the hydration number and distance in the  $0.98 \text{ kmol m}^{-3}$   $ZnCl_2$  solution of the present study appear rather to support the results of the conventional x-ray scattering technique. Namely, the hydration number of  $Zn^{2+}$  is about 6 and the distance between  $Zn^{2+}$  and  $OH_2$  is about 0.210 nm [1–6]. A slight increase in these values of the hydration number and distance was observed in the  $2.85 \text{ kmol m}^{-3}$   $ZnCl_2$  solution. Although the error due to counting statistics is less than 0.5% in the present measurements, it increases up to about 8% by taking the difference between these observed intensities. As a result, the error of the reduced environmental RDF  $G_{Zn}(r)$  becomes about 15% at most. If these errors are taken into account, the difference of the hydration numbers and distances between the solutions is insignificant. In order to investigate a slight change of the structure around the  $Zn^{2+}$  ions, if any, it is necessary to carry out systematic AXS measurements of the solutions over a wider concentration range from low concentration to saturation. This is beyond the scope of the present study.

In conclusion, the  $Zn^{2+}$  is coordinated by 5.8  $OH_2$  molecules in the solution for concentrations up to at least  $1 \text{ kmol m}^{-3}$   $ZnCl_2$ , and the essential configuration around  $Zn^{2+}$  does not show any significant difference even in a solution of about  $3 \text{ kmol m}^{-3}$   $ZnCl_2$ . It should also be noted that the possible interpretation of the data by postulating the formation of some kind of complexes containing  $Cl^-$  around  $Zn^{2+}$  is not excluded in the present study. The potential capability of the AXS technique to investigate the



structure around a heavy metal cation in aqueous solutions has been clearly demonstrated and the present authors maintain the view that the AXS technique is very promising for structural characterisation of dilute aqueous solution such as  $\text{ZnCl}_2$ , corresponding to the 0.6 at. %  $\text{Zn}^{2+}$ , as shown by the present work.

### Acknowledgments

A part of this research was supported by the Mitsubishi Foundation on the research project of the anomalous x-ray scattering in 1986. We (EM and YW) particularly want to thank the staff of Photon Factory, National Laboratory for High Energy Physics, Drs T Ishikawa, M Nomura and A Koyama, and Professors T Matsushita, H Iwasaki and M Ando. Dr S Kudo provided valuable advice and assistance regarding sample preparation.

### References

- [1] Wertz D L, Lawrence R M and Kruh R F 1965 *J. Chem. Phys.* **43** 2163
- [2] Wertz D L and Kruh R F 1969 *J. Chem. Phys.* **50** 4313
- [3] Ohtaki H, Yamaguchi T and Maeda M 1976 *Bull. Chem. Soc. Japan* **49** 701
- [4] Caminiti R and Cucca P 1982 *Chem. Phys. Lett.* **89** 110
- [5] Howe R A, Hawells W S and Enderby J E 1974 *J. Phys. C: Solid State Phys.* **7** L111
- [6] Neilson G W and Enderby J E 1978 *J. Phys. C: Solid State Phys.* **11** L625
- [7] Fontana M P, Maisano G, Migliardo P and Wanderlingh F 1977 *Solid State Commun.* **23** 489
- [8] Sandstrom D R 1979 *J. Chem. Phys.* **71** 2381
- [9] Lagarde P, Fontaine A, Raoux D, Sadoc A and Migliardo P 1980 *J. Chem. Phys.* **72** 3061
- [10] Ludwig K F Jr, Warburton W K and Fontaine A 1987 *J. Chem. Phys.* **87** 620
- [11] Dreier P and Rabe P 1986 *J. Physique* **47** C8 809
- [12] Waseda Y 1981 *Prog. Mater. Sci.* **26** 1
- [13] Waseda Y, Matsubara E and Sugiyama K 1988 *Sci. Rep. Res. Inst. Tokohu Univ.* **A 34** 1
- [14] Matsubara E, Waseda Y, Mitera M and Masumoto T 1988 *Trans. Japan Inst. Met.* **29** 697
- [15] Aur S, Kofalt D, Waseda Y, Egami T, Wang R, Chen H S and Teo B K 1983 *Solid State Commun.* **48** 111
- [16] Rao N V, Reddy S B, Satyanarayana G and Sastry D L 1986 *Physica C* **138** 215
- [17] Waseda Y 1984 *Novel Application of Anomalous X-ray Scattering for Structural Characterization of Disordered Materials* (New York: Springer) p 84
- [18] Wagner C N J, Ocken H and Joshi M L 1965 *Z. Naturf.* **a 20** 325
- [19] *International Tables for X-ray Crystallography* 1974, vol. 4 (Birmingham: Kynock) p 99
- [20] Cromer D T and Libermann D 1970 *J. Chem. Phys.* **53** 1891
- [21] *International Tables for X-ray Crystallography* 1968 vol 3 (Birmingham: Kynock) p 250
- [22] Compton A H and Allison S K 1967 *X-rays in Theory and Experiment* 2nd ed. (Toronto: Van Nostrand) p 782
- [23] Morimoto H 1958 *J. Phys. Soc. Japan* **13** 1015
- [24] Furukawa K 1962 *Rep. Prog. Phys.* **25** 395
- [25] Hosoya S 1970 *Bull. Phys. Soc. Japan* **25** 110
- [26] Shevchik N J 1977 *Phil. Mag.* **35** 805
- [27] Fuoss P H, Eisenberger P, Warburton W K and Biedenstock A 1981 *Phys. Rev. Lett.* **46** 1537
- [28] Neilson G W, Howe R A and Enderby J E 1975 *Chem. Phys. Lett.* **33** 284
- [29] Neilson G W and Enderby J E 1983 *Proc. R. Soc. A* **390** 353
- [30] Narten A H and Levy H A 1969 *Science* **165** 447
- [31] Enderby J E and Neilson G W 1980 *Adv. Phys.* **29** 323
- [32] Matsubara E, Waseda Y, Ashizuka M and Ishida E 1988 *J. Non-Cryst. Solids* **103** 117
- [33] Greenfield A J, Wellendorf J and Wiser N 1971 *Phys. Rev. A* **4** 1607
- [34] Bol W, Gerrits G J A and van Panthaleon van Eck C L 1970 *J. Appl. Cryst.* **3** 486